

Absolute configuration of the diterpenoids icetexone and conacytone from *Salvia ballotaeflora*

Baldomero Esquivel¹ | Eleuterio Burgueño-Tapia² | Celia Bustos-Brito¹ |
Nury Pérez-Hernández³ | Leovigildo Quijano¹ | Pedro Joseph-Nathan⁴ 

¹Instituto de Química, Universidad Nacional Autónoma de México, Ciudad Universitaria, Mexico City, Mexico

²Departamento de Química Orgánica, Escuela Nacional de Ciencias Biológicas, Instituto Politécnico Nacional, Mexico City, Mexico

³Escuela Nacional de Medicina y Homeopatía, Instituto Politécnico Nacional, Mexico City, Mexico

⁴Departamento de Química, Centro de Investigación y de Estudios Avanzados del Instituto Politécnico Nacional, Mexico City, Mexico

Correspondence

Pedro Joseph-Nathan, Departamento de Química, Centro de Investigación y de Estudios Avanzados del Instituto Politécnico Nacional, Apartado 14-740, Mexico City 07000, Mexico.
Email: pjoseph@nathan.cinvestav.mx

Abstract

Detailed literature inspections regarding the diterpenoids icetexone (**1**) and conacytone (**3**) reveal that the absolute configuration (AC) of these natural occurring compounds is not rigorously proven, despite they were originally isolated in 1976. This task is now completed by single-crystal X-ray diffraction Flack and Hooft parameters determination after processing data collected with Cu $K\alpha$ graphite monochromated radiation. The AC of both compounds is further determined by vibrational circular dichroism measurements performed on icetexone acetate (**2**) and conacytone triacetate (**4**) since the solubility of **1** and **3** is limited. Comparison of the substituent chemical shifts (SCS) induced by acetylation of **1** and **3** to afford **2** and **4**, respectively, reveals that in the case of icetexone, all six SCS values of the quinone ring are in excellent agreement with the expected values, while in the case of conacytone, three agree and three do not agree due to the presence of additional acetates near the quinone ring. Density functional theory calculations performed on 3-hydroxythymoquinone (**6**) and its tautomer 4-hydroxy-1,2-quinone **7**, on 6-hydroxythymoquinone (**8**) and its tautomer *ortho*-quinone **9**, and on icetexone (**1**) and the claimed natural occurring *ortho*-quinone tautomer romulogarzone (**5**) indicate that 2-hydroxy-1,4-quinones are more stable, by some 11–14 kcal/mol, than their 4-hydroxy-1,2-quinone tautomers, and therefore, romulogarzone (**5**) is inexistent.

KEYWORDS

absolute configuration, Flack parameters, Hooft parameters, hydroxy-*p*-benzoquinones, single-crystal X-ray diffraction, substituent chemical shift parameters, vibrational circular dichroism

1 | INTRODUCTION

Common triterpenoids and sitosterol,¹ as well as icetexone (**1**) and conacytone (**3**), were isolated² from *Salvia ballotaeflora* over 40 years ago. They took their names in recognition to ICETEX, a Colombian student-ship agency,¹ and to CONACYT, the National Science and Technology Council of Mexico, respectively. The

structure and relative stereochemistry of **1** followed from single-crystal X-ray diffraction analyses, whose data³ allowed to refine the structure to $R = 3.7\%$. Another paper⁴ further describes a third compound, romulogarzone, which is postulated as the *ortho*-quinone **5** without rigorous structure proof either by X-ray analysis or by chemical correlation of **1** and **5** through a common leucotriacetate derivative, if as a prerequisite **1**

and **5** would show depression in a mixed melting point determination. The structure of **3** also followed⁵ from X-ray data, while for **5**, no further isolation report is available since then. Ictexone (**1**)²⁻⁴ appeared also in *Salvia anastomosans*,⁶ *Salvia candicans*,⁷ and *Salvia pubescens*.⁸

An approach to the absolute configuration of icetexone (**1**) followed from an asymmetric total synthesis.⁹ The structure was verified by single-crystal X-ray diffraction analysis for which the unit cell parameters agree with those published³ in 1976, thereby establishing the identity of **1** from both natural and synthetic origins, although the original X-ray paper³ seems to be overlooked for such a comparison.⁹ It is clear from the asymmetric synthesis that icetexone is properly represented as shown in **1**, but it might be inferred that the natural occurring diterpenoid would be the enantiomer since for synthetic **1** $[\alpha]_{\text{D}} -70$, in chloroform, is reported,⁹ while for the natural sample $[\alpha]_{\text{D}} +33.3$, also in chloroform, is given.^{2,4}

In another paper¹⁰ on the enantioselective formal synthesis of icetexone, the authors indicate that “X-ray crystallographic analysis enabled a determination of the absolute configuration of **1**” in the 1976 X-ray paper.³ This affirmation is incorrect since at those times, the only way to determine an absolute configuration by single-crystal X-ray diffraction (XRD) analysis was by anomalous dispersion caused by the presence of a heavy atom, like a bromine atom, in the studied molecule.

In turn, conacytone (**3**) was also isolated from *S pubescens*,¹¹ *S anastomosans*,⁶ *S candicans*,⁷ and from another collection of *S ballotaeflora*.¹²

In summary, the absolute configuration of natural occurring icetexone (**1**) and conacytone (**3**) is not rigorously proven, and their NMR data remain to be assigned. Therefore, in the present paper, we describe a full account regarding the three terpenoids **1**, **3**, and **5** originally reported²⁻⁵ in 1976.

2 | MATERIALS AND METHODS

2.1 | General

Melting points were determined on a Fisher-Jhons apparatus and are uncorrected. Optical rotations were measured on a Perkin-Elmer (Boston, MA) 341 polarimeter. Nuclear magnetic resonance (NMR) measurements were performed on Varian (Palo Alto, CA) Mercury 300 spectrometers. Chemical shifts were referred to tetramethylsilane (TMS). Infrared (IR) and vibrational circular dichroism (VCD) spectra were measured using a BioTools (Jupiter, FL) dual PEM ChiralIR FT-VCD spectrophotometer. Single-crystal X-ray diffraction

measurements (XRD) were performed on an Agilent (Santa Clara, CA) Xcalibur Atlas Gemini diffractometer.

2.2 | Compounds

Samples of icetexone (**1**) and conacytone (**3**) were available from previous studies,^{8,12} while icetexone acetate (**2**) and conacytone triacetate (**4**) were obtained by acetylation of the natural products using standard reaction conditions.

2.2.1 | Ictexone (1)

Orange-red prisms, mp 260-264 °C dec. $[\alpha]_{589} -94.1$, $[\alpha]_{578} -95.0$ (*c* 0.56, CHCl₃). ¹H NMR δ 7.11 (1H, s, OH), 6.86 (1H, dd, *J* = 12.3, 2.0 Hz, H-7), 6.43 (1H, dd, *J* = 12.3, 5.0 Hz, H-6), 3.22 (1H, hept, *J* = 7.0 Hz, H-15), 3.16 (1H, d, *J* = 13.9 Hz, H-20), 2.79 (1H, d, *J* = 13.9 Hz, H-20'), 2.55 (1H, dd, *J* = 5.0, 2.0 Hz, H-5), 2.01 (1H, m, H-1), 1.81 (3H, m, H-1', H-2, H-2'), 1.77 (1H, m, H-3), 1.62 (1H, m, H-3'), 1.26 (3H, s, H-18), 1.24 (3H, d, *J* = 7.0 Hz, H-17), 1.23 (3H, d, *J* = 7.0 Hz, H-16). ¹³C NMR δ 185.6 (C-14), 182.8 (C-11), 178.8 (C-19), 150.8 (C-12), 140.5 (C-8), 138.7 (C-6), 133.6 (C-9), 125.4 (C-7), 125.1 (C-13), 92.3 (C-10), 57.7 (C-5), 47.7 (C-4), 35.9 (C-3), 35.6 (C-1), 32.7 (C-20), 24.4 (C-15), 19.9 (C-16), 19.8 (C-17), 19.5 (C-2), 18.2 (C-18).

2.2.2 | Ictexone acetate (2)

Yellow needles, mp 159-162 °C. $[\alpha]_{589} -211.3$, $[\alpha]_{578} -222.5$, $[\alpha]_{546} -255.5$ (*c* 0.53, CHCl₃). ¹H NMR δ 6.78 (1H, dd, *J* = 12.1, 2.2 Hz, H-7), 6.47 (1H, dd, *J* = 12.1, 4.7 Hz, H-6), 3.17 (1H, hept, *J* = 7.0 Hz, H-15), 2.97 (1H, d, *J* = 13.6 Hz, H-20), 2.91 (1H, d, *J* = 13.6 Hz, H-20'), 2.48 (1H, dd, *J* = 4.7, 2.2 Hz, H-5), 2.36 (3H, s, Ac), 1.96 (1H, m, H-1), 1.78 (2H, m, H-2, H-2'), 1.77 (2H, m, H-1', H-3), 1.58 (1H, m, H-3'), 1.27 (3H, s, H-18), 1.24 (3H, d, *J* = 7.0 Hz, H-17), 1.22 (3H, d, *J* = 7.0 Hz, H-16). ¹³C NMR δ 185.4 (C-14), 179.2 (C-11), 178.7 (C-19), 168.2 (Ac C=O), 148.9 (C-12), 140.5 (C-13), 139.9 (C-8), 138.3 (C-6), 137.0 (C-9), 125.4 (C-7), 94.5 (C-10), 56.9 (C-5), 47.3 (C-4), 35.9 (C-3), 34.9 (C-1), 33.3 (C-20), 25.5 (C-15), 20.4 (Ac Me), 20.4 (C-16), 20.3 (C-17), 19.4 (C-2), 17.9 (C-18).

2.2.3 | Conacytone (3)

Yellow prisms, mp 217-219 °C dec. $[\alpha]_{589} -37.0$, $[\alpha]_{578} -52.3$, $[\alpha]_{546} -124.4$ (*c* 1.0, CHCl₃). ¹H NMR see Table 1. ¹³C NMR δ 188.8 (C-14), 183.9 (C-11), 151.0 (C-12), 145.1 (C-8), 142.5 (C-9), 124.7 (C-13), 95.3 (C-20), 66.2 (C-19), 62.2 (C-7), 41.6 (C-10), 40.0 (C-5), 39.9 (C-3), 34.9

TABLE 1 Accurate ^1H NMR data of conacytone (**2**) obtained from very high-resolution 300 MHz measurements and PERCH iterations

Atom	^1H	Mult	J
1 α	1.312	ddd	$^2J_{1\alpha,1\beta} = -13.11$, $^3J_{1\alpha,2\alpha} = 6.10$, $^3J_{1\alpha,2\beta} = 13.72$
1 β	2.558	ddd	$^2J_{1\alpha,1\beta} = -13.11$, $^3J_{1\beta,2\alpha} = 1.29$, $^3J_{1\beta,2\beta} = 5.89$
2 α	1.599	dddd	$^3J_{1\alpha,2\alpha} = 6.10$, $^3J_{1\beta,2\alpha} = 1.29$, $^2J_{2\alpha,2\beta} = -13.52$, $^3J_{2\alpha,3\alpha} = 6.85$, $^3J_{2\alpha,3\beta} = 0.73$
2 β	2.432	dddd	$^3J_{1\alpha,2\beta} = 13.72$, $^3J_{1\beta,2\beta} = 5.89$, $^2J_{2\alpha,2\beta} = -13.52$, $^3J_{2\beta,3\alpha} = 13.68$, $^3J_{2\beta,3\beta} = 6.28$
3 α	1.469	dddd	$^3J_{2\alpha,3\alpha} = 6.85$, $^3J_{2\beta,3\alpha} = 13.68$, $^2J_{3\alpha,3\beta} = -13.12$, $^4J_{3\alpha,19R} = 2.66$
3 β	1.754	dddd	$^3J_{2\alpha,3\beta} = 0.73$, $^3J_{2\beta,3\beta} = 6.28$, $^2J_{3\alpha,3\beta} = -13.12$
5	1.725	ddd	$^3J_{5,6\alpha} = 2.96$, $^3J_{5,6\beta} = 14.19$, $^4J_{5,19S} = 1.43$
6 α	1.880	ddd	$^3J_{5,6\alpha} = 2.96$, $^2J_{6\alpha,6\beta} = -13.65$, $^3J_{6\alpha,7} = 1.64$
6 β	2.300	ddd	$^3J_{5,6\beta} = 14.19$, $^2J_{6\alpha,6\beta} = -13.65$, $^3J_{6\beta,7} = 4.59$
7	4.836	ddd	$^3J_{6\alpha,7} = 1.64$, $^3J_{6\beta,7} = 4.59$, $^3J_{7,\text{OH}} = 2.54$
OH-7	2.220	d	$^3J_{7,\text{OH}} = 2.54$
OH-12	7.190	s	-
15	3.192	qq	$^3J_{15,16} = 7.08$, $^3J_{15,17} = 7.08$
16	1.240	d	$^3J_{15,16} = 7.08$
17	1.235	d	$^3J_{15,17} = 7.08$
18	0.826	s	-
19R	3.877	dd	$^4J_{3\alpha,19R} = 2.66$, $^2J_{19R,19S} = -11.24$
19S	3.349	dd	$^4J_{5,19S} = 1.43$, $^2J_{19R,19S} = -11.24$,
20	5.601	d	$^3J_{20,\text{OH}} = 2.05$
OH-20	2.858	d	$^3J_{20,\text{OH}} = 2.05$

(C-1), 32.5 (C-4), 26.2 (C-6), 24.1 (C-15), 23.6 (C-18), 21.1 (C-2), 19.9 (C-16), 19.8 (C-17).

2.2.4 | Conacytone triacetate (**4**)

Oil. $[\alpha]_{589} +59.4$, $[\alpha]_{578} +59.3$, $[\alpha]_{546} +53.2$, (c 0.91, CHCl_3). ^1H NMR δ 6.58 (1H, s, H-20), 6.09 (1H, dd, $J = 4.3$, 1.9 Hz, H-7), 3.68 (1H, dd, $J = 11.3$, 2.5 Hz, H-19), 3.45 (1H, dd, $J = 11.3$, 1.3 Hz, H-19'), 3.13 (1H, hept, $J = 7.1$ Hz, H-15), 2.55 (1H, br-dd, $J = 13.0$, 6.1 Hz, H-1), 2.43 (1H, qd, $J = 13.0$, 6.3 Hz, H-2), 2.33 (3H, s, Ac-12), 2.24 (1H, td, $J = 14.4$, 4.3 Hz, H-6), 2.07 (3H, s, Ac-7). 1.93 (1H, ddd, $J = 14.4$, 2.8, 1.9 Hz, H-6'), 1.89 (3H, s, Ac-20), 1.78 (1H, br-dd, $J = 13.2$, 6.1, 1.3 Hz, H-3), 1.65 (1H, dd, 14.4, 2.8, H-5), 1.63 (1H, m, H-2'), 1.46 (1H, tdd, $J = 13.2$, 6.3, 2.5 Hz, H-3), 1.43 (1H, td, $J = 13.1$, 6.0 Hz, H-1'), 1.21 (3H, $J = 7.1$, H-16), 1.20 (3H, $J = 7.1$, H-16), 0.78 (3H, s, H-18). ^{13}C NMR δ 185.1 (C-14), 180.2 (C-11), 169.6 (Ac 7 C=O), 168.9 (Ac 20 C=O), 168.2 (Ac 12 C=O), 149.2 (C-12), 146.5 (C-8), 139.9 (C-9), 139.8 (C-13), 94.3 (C-20), 67.3 (C-19), 62.8 (C-7), 41.2 (C-10), 40.4 (C-5), 39.9 (C-3), 34.8 (C-1), 32.2 (C-4), 25.2 (C-15), 25.1 (C-6), 23.5 (C-18), 21.1 (2C, Ac 7 and 20 Me), 20.9 (C-2), 20.4 (Ac 12 Me) 20.3 (C-16), 20.2 (C-17).

2.3 | Single-crystal X-ray diffraction analysis

Crystals of icetexone (**1**) and conacytone (**3**) were mounted on glass fibers for data collection using Cu $K\alpha$ graphite monochromated radiation ($\lambda = 1.54184 \text{ \AA}$) at 293(2) K in the $\omega/2\theta$ scan mode. In the case of **1**, an orange-red crystal measuring $0.15 \times 0.10 \times 0.08 \text{ mm}$, $\text{C}_{20}\text{H}_{22}\text{O}_5$, $M = 342.38$ turned out to be orthorhombic, space group $P2_12_12_1$, $a = 7.7453(3) \text{ \AA}$, $b = 10.3664(3) \text{ \AA}$, $c = 21.0064(7) \text{ \AA}$, $V = 1686.6(1) \text{ \AA}^3$, $Z = 4$, $\rho = 1.348 \text{ mg/mm}^3$, $\mu = 0.790 \text{ mm}^{-1}$, total reflections 17 373, unique reflections 2904 ($R_{\text{int}} 0.044$), observed reflections 2436. In the case of **3**, a yellow crystal measuring $0.41 \times 0.37 \times 0.51 \text{ mm}$, $\text{C}_{20}\text{H}_{26}\text{O}_6$, $M = 362.41$ also turned out to be orthorhombic, space group $P2_12_12_1$, $a = 10.956(1) \text{ \AA}$, $b = 12.635(1) \text{ \AA}$, $c = 13.602(2) \text{ \AA}$, $V = 1882.9(4) \text{ \AA}^3$, $Z = 4$, $\rho = 1.278 \text{ mg/mm}^3$, $\mu = 0.773 \text{ mm}^{-1}$, total reflections 13 780, unique reflections 3208 ($R_{\text{int}} 0.038$), observed reflections 2599. Either structure was solved by direct methods using the SHELXS-97 program included in the WinGX v1.70.01 crystallographic software package.¹³ For the structural refinement, the non-hydrogen atoms were treated anisotropically, and the hydrogen atoms, included in the structure factor calculations, were refined isotropically. The final R indices for **1** were $[I > 2\sigma(I)]$

$R_1 = 3.3\%$ and $wR_2 = 6.8\%$, largest difference peak and hole, 0.129 and $-0.110 \text{ e.}\text{\AA}^3$, and those for **3** were $[I > 2\sigma(I)] R_1 = 3.4\%$ and $wR_2 = 7.0\%$, largest difference peak and hole, 0.131 and $-0.116 \text{ e.}\text{\AA}^3$. The Olex2 v1.1.5 software¹⁴ allowed calculating the Flack¹⁵ (x) and Hooft (y) parameters.^{16,17} In the case of **1**, these parameters were $x = 0.04(19)$ and $y = 0.12(9)$, which for the inverted structure were $x = 0.95(19)$ and $y = 0.88(9)$, while for **3**, they were $x = 0.00(18)$ and $y = 0.05(9)$, which again for the inverted structure were $x = 0.99(18)$ and $y = 0.94(9)$. Crystallographic data (excluding structure factors) have been deposited at the Cambridge Crystallographic Data Centre, from where copies of the data can be obtained free of charge on application to the CCDC, Cambridge, UK. The CCDC deposition numbers are 1562319 and 1562343 for **1** and **3**, respectively, and PLUTO representations of both X-ray structures are shown in Figure 1.

2.4 | VCD measurements

Samples of 3.4 mg of **2** and 5.5 mg of **4** dissolved in 100 μl of 100% atom-D CDCl_3 were placed in a cell with BaF_2 windows and a path length of 0.1 mm for data acquisition at a resolution of 4 cm^{-1} over 5 h. A baseline correction was performed by subtracting the spectrum of the solvent acquired under identical conditions. The samples stability

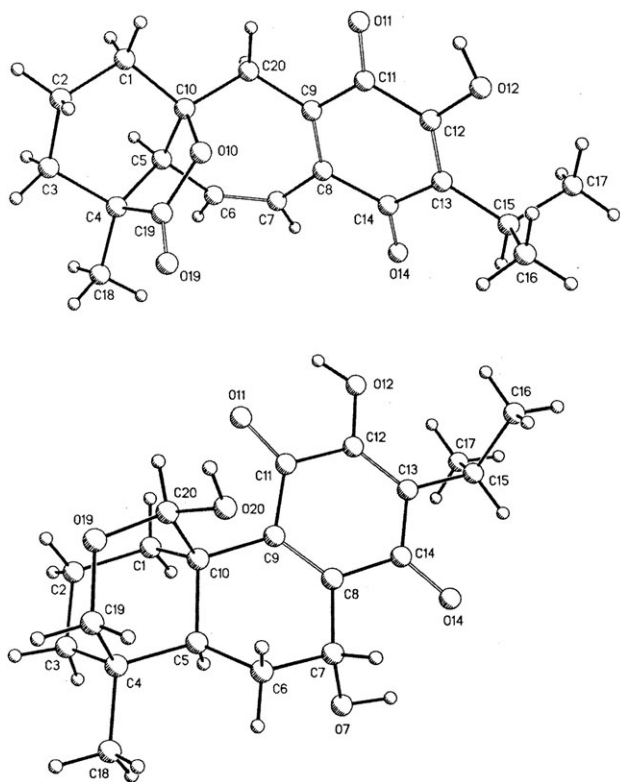


FIGURE 1 PLUTO X-ray structure plots of icetexone (**1**, top) and conacytone (**3**, bottom)

was monitored in either case by ^1H NMR analysis immediately before and after the VCD measurements.

2.5 | Computational methods

The molecular models of **2** and **4** were built with the Spartan 08 (Wavefunction, Inc, Irvine, CA) software, and their initial conformational searches were carried out using the Monte Carlo protocol and molecular mechanic force field (MMFF94) calculations in an energy windows of 10 kcal/mol. In the case of **2**, starting from B-ring bowl- and dome-shaped conformers, this procedure provided four structures in each case, while for **4**, it gave 12 conformers in a 6.92 kcal/mol energy gap. Single-point DFT calculations of all conformers were done using the B3LYP functional and the 6-31G(d) basis set implemented in the same software package, which retained the eight conformers for **2** in a 2.70 kcal/mol energy range and provided six conformers for **4** in a 1.82 kcal/mol interval, the next conformer being 4.18 kcal/mol over the global minimum. Further conformational optimizations were performed using the Gaussian 03 (Gaussian, Inc, Wallingford, CT) software to provide the thermochemical parameters summarized in Table 2. For calculating final vibrational normal modes and rotational strengths, using DFT at the B3LYP/DGDZVP level of theory, the value of ΔG was estimated for each conformer and used as a criterion for weighting the IR and VCD spectra for **2** and **4**. Finally, eight conformers for **2** and four for **4** were found within 0.75 and 1.16 kcal/mol energy gaps, respectively. The band shapes were generated with Lorentzian functions and a bandwidth of 6 cm^{-1} . Calculated and experimental spectra were compared using the CompareVOA (BioTools, Jupiter, FL) software,¹⁸ the pertinent parameters being shown in Table 3. The final graphical comparison of experimental and calculated IR and VCD spectra, shown in Figures 2 and 3 for **2** and **4**, respectively, was prepared using eight and four conformers. The four minimum energy conformers for icetexone acetate (**2**) and conacytone triacetate (**4**) are shown in Figure 4.

For the tautomers equilibria calculations of **1** versus **5**, of **6** versus **7**, and of **8** versus **9**, the molecular models were also constructed in the Spartan 08 suite, followed by Monte Carlo MMFF94 calculations, to provide two relevant conformers for the *para*-quinones **1**, **6**, and **8**, while for the *ortho*-quinones **5**, **7**, and **9**, four conformers were provided. In all cases, single-point calculations using DFT at the B3LYP/DGDZVP level of theory were performed using the Spartan 08 software, followed by further conformational optimization using the Gaussian 03 software to provide the thermochemical parameters given in Table 4. In order to calculate vibrational normal modes, DFT calculations at the same level of theory provided

TABLE 2 Thermochemical parameters for quinones **2** and **4**

Compound	$\Delta E_{\text{MMFF}}^{\text{a}}$	% ^b	$\Delta E_{6-31\text{G(d)}}^{\text{c}}$	% ^b	$\Delta E_{\text{DGDZVP}}^{\text{d}}$	% ^b	$\Delta G_{\text{DGDZVP}}^{\text{e}}$	% ^f
2a	0.00	49.1	0.00	69.3	0.00	36.5	0.00	30.1
2b	0.66	16.1	1.06	11.6	0.56	14.2	0.38	16.0
2c	0.97	9.6	1.29	7.9	0.47	16.5	0.40	15.4
2d	0.79	12.9	1.62	4.5	0.75	10.2	0.61	10.7
2e	1.38	4.8	2.70	0.7	1.26	4.4	0.75	8.4
2f	1.67	2.9	2.35	1.3	0.94	7.5	0.82	7.6
2g	1.56	3.5	1.65	4.2	0.92	7.7	0.88	6.8
2h	2.18	1.1	2.94	0.5	1.48	3.0	1.06	5.0
4a	0.00	77.7	0.10	31.7	0.00	47.8	0.00	45.9
4b	0.86	18.2	1.10	5.9	0.21	33.6	0.11	38.1
4c	2.01	2.6	1.52	2.9	-	-	-	-
4d	2.88	0.7	0.00	37.5	0.93	10.0	0.93	9.6
4e	2.89	0.6	1.82	1.7	1.01	8.6	1.16	6.4
4f	3.66	0.2	1.37	20.3	-	-	-	-

^aRelative to **2a** (67.25 kcal/mol) and **4a** (26.7 kcal/mol).

^bCalculated using $\Delta E \cong -RT \ln K$.

^cRelative to **2a** (-818 355.28 kcal/mol) and **4d** (-1 058 648.06 kcal/mol).

^dRelative to **2a** (-818 457.32 kcal/mol) and **4a** (-1 058 788.93 kcal/mol).

^eRelative to **2a** (-818 225.61 kcal/mol) and **4a** (-1 058 485.16 kcal/mol).

^fCalculated using $\Delta G = -RT \ln K$.

TABLE 3 Confidence level data for the IR and VCD spectra comparison of **2** and **4**

Compound	anH^{a}	S_{IR}^{b}	S_{E}^{c}	S_{-E}^{d}	ESI^{e}	C^{f}
2	0.984	98.1	76.8	14.8	62.0	100
4	0.989	86.7	71.3	16.8	54.5	100

^aAnharmonicity factor.

^bIR spectral similarity in percentage.

^cVCD spectral similarity for the correct enantiomer in percentage.

^dVCD spectral similarity for the opposite enantiomer in percentage.

^eEnantiomer similarity index, calculated as the $S_{\text{E}} - S_{-E}$ difference.

^fConfidence level for the absolute configuration determination in percentage.

the free energy values that allowed comparing the tautomer pairs **1/5**, **6/7**, and **8/9**.

3 | RESULTS AND DISCUSSION

The reported ambiguities for solid icetexone (**1**), as orange-red crystals,³ as orange crystals,² or as yellow crystals,⁴ opened the possibility that **1** might show polymorphs, as we recently found for an isoflavone.¹⁹ Thus, careful evaluation of the behavior of **1** revealed that slow crystallization from chloroform, or from chloroform-acetone solutions, provided orange-red prisms, while fast

evaporation of these solutions provided orange powder. In neither case, after many other manipulation trials, could we obtain yellow crystals of **1**. Another point in need of clarification is the mp behavior of **1**, which in the 1976 papers^{2,4} is reported as 226-227 °C, while in the asymmetric synthesis paper,⁹ it is reported as 247-253 °C. In our hands, orange-red prisms of **1**, upon heating to around 230 °C, show a solid state transition to an orange solid which at around 257 °C start to darken and melt at 260-264 °C to leave a dark brown liquid. In turn, the reported optical activity data of **1** are also confusing, since the original 1976 paper² states $[\alpha]_{\text{D}} +33.3$ (*c* 1.0, CHCl₃), while the asymmetric synthesis paper indicates $[\alpha]_{\text{D}} -70$ (*c* 0.65, CHCl₃), thereby opening the possibility that the synthesized sample of icetexone would be the enantiomer of the natural product. In our hands, the optical activity value of natural **1** was $[\alpha]_{\text{D}} -94.1$ (*c* 0.56, CHCl₃). In the case of icetexone acetate (**2**), the original paper⁴ provides no optical activity data and indicates mp 248-250 °C, which seems quite peculiar since for natural product **1**, it indicates mp 226-227 °C. In our hands, acetate **2** showed mp 159-162 °C and a strong $[\alpha]_{589}$ value of -211.3.

Since crystals of icetexone (**1**) have been diffracted twice,^{3,9} a secure way to know that the absolute configuration of this diterpenoid was by determining the crystal structure again, but this time using graphite

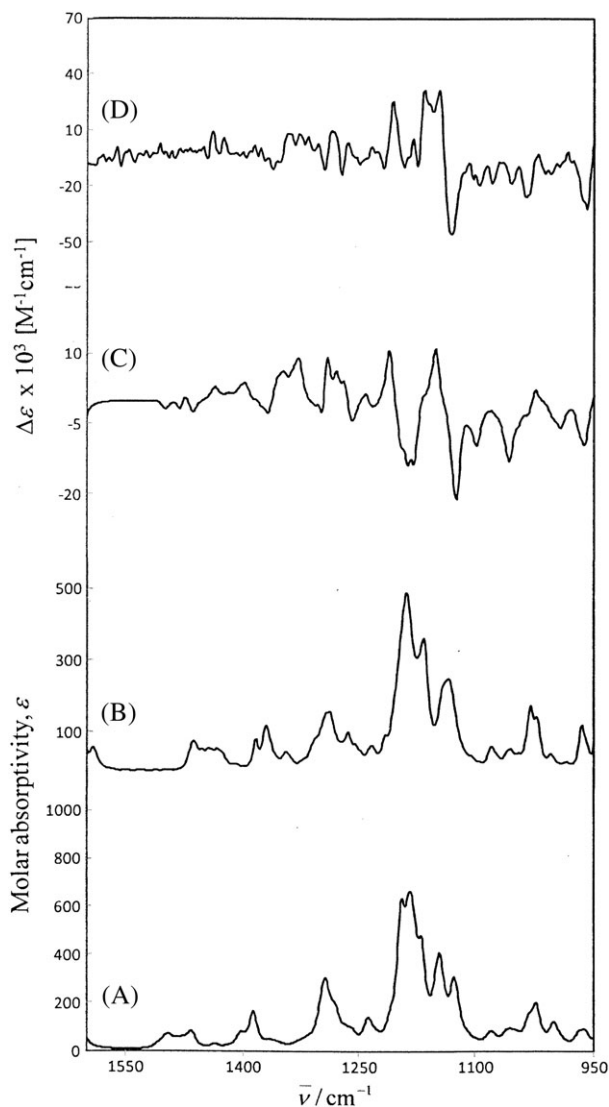


FIGURE 2 Comparison of the experimental (B) IR and (D) VCD spectra of icetexone acetate (**2**) with the DFT B3LYP/DGDZVP calculated (A) IR and (C) VCD spectra for (4*S*,5*S*,10*S*)-**2**

monochromated Cu $K\alpha$ radiation which allows to calculate Flack and Hooft parameters, thereby providing conclusive absolute configuration evidence. Thus, a crystal of **1** was diffracted giving cell parameters in agreement with those reported.^{3,9} The molecular structure could nicely be refined to $R = 3.3\%$, and the Flack¹⁵ $x = 0.04(19)$ and Hooft^{16,17} $y = 0.12(9)$ parameters gave the absolute configuration depicted in **1**. A PLUTO representation of the molecule is given in Figure 1, and as a complementary absolute configuration X-ray test, the Flack and Hooft parameters for the enantiomer were $x = 0.95(19)$ and $y = 0.88(9)$.

In the case of conacytone (**3**), there is also a mp inconsistency in the 1976 papers, since in one case,² mp = 240 °C is reported, while in another case,⁴ the range 210–212 is given. Our measurements indicate that it shows

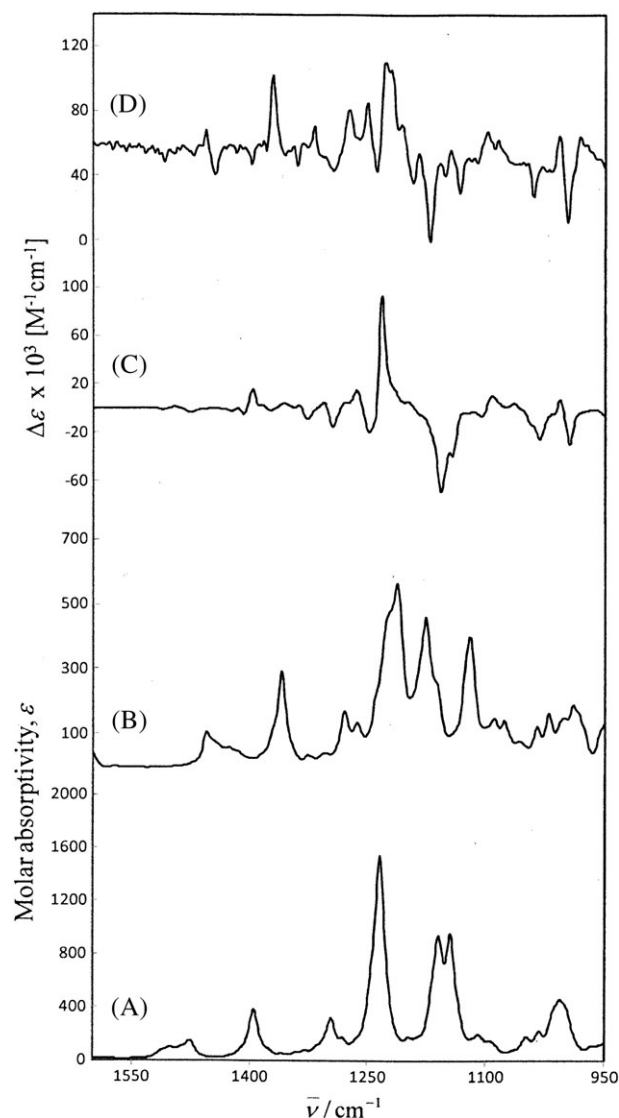


FIGURE 3 Comparison of the experimental (B) IR and (D) VCD spectra of conacytone triacetate (**4**) with the DFT B3LYP/DGDZVP calculated (A) IR and (C) VCD spectra for (4*S*,5*S*,7*R*,10*R*,20*S*)-**4**

mp 217–219 °C. Compound **3** is a less studied molecule, for which, in addition to the original 1976 papers,^{2,4,5} only isolation reports are available in the literature.^{6,7,11,12} An X-ray diffracted crystal also provided cell parameters in agreement with those reported,⁵ the solid state structure was refined to $R = 3.4\%$, and the Flack $x = 0.00(18)$ and Hooft $y = 0.05(9)$ parameters for the correct enantiomer, whose PLUTO plot is shown in Figure 1, provided the absolute configuration. Complementary to the absolute configuration determination, the parameters for the inverted structure were $x = 0.99(18)$ and $y = 0.94(9)$.

In order to gain independent evidence for the absolute configuration of icetexone (**1**) and conacytone (**3**), we selected vibrational circular dichroism (VCD) as the methodology of choice, which has been used extensively for the study of diterpenoids.^{20,21} For this purpose, there

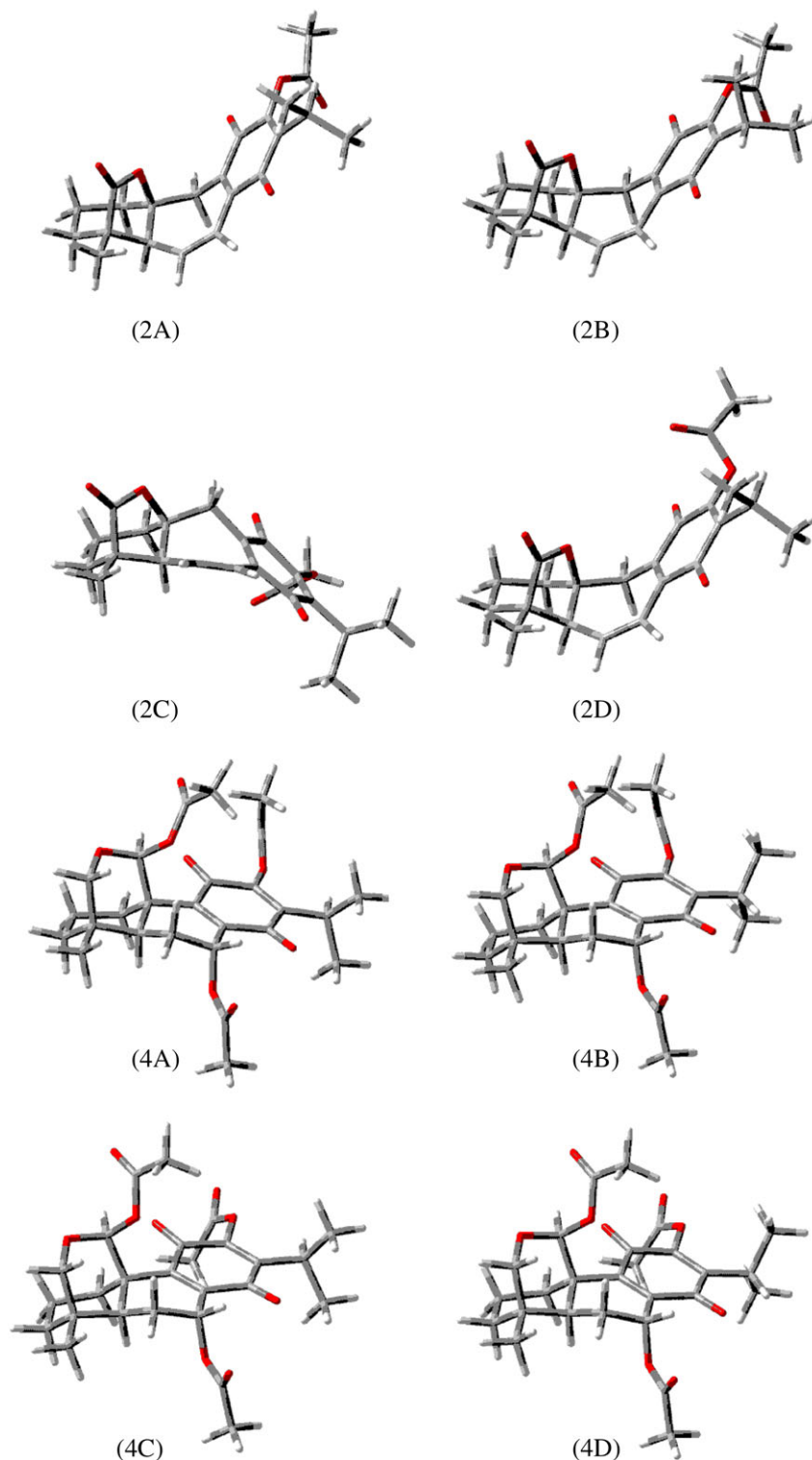


FIGURE 4 Minimum energy conformers of icetexone acetate (**2**) and of conacytone triacetate (**4**)

were a couple difficulties to overcome, which are the low solubility of either natural product in chloroform, a solvent extensively used in such studies, and the presence of two secondary non-hydrogen bonded hydroxy groups in **3** which could be prone for intermolecular associations in solution, thereby complicating the comparison task of the experimental VCD spectra with those obtained by density functional theory (DFT) calculations.^{22,23}

Therefore, the VCD studies were performed using icetexone acetate (**2**) and conacytone triacetate (**4**), both obtained after routine acetylation of the two natural products.

Assembly of a solid Dreiding stereomodel from Büchi (Flawil, Switzerland) revealed that for icetexone acetate (**2**), the seven-membered ring can adopt either a bowl or a dome shape, and that the conformational interconversion

TABLE 4 Thermochemical parameters for quinones **1** and **5-9**

Compound	$\Delta E_{\text{MMFF}}^{\text{a}}$	% ^b	$\Delta E_{6-31\text{G(d)}}^{\text{c}}$	% ^b	$\Delta E_{\text{DGDZVP}}^{\text{d}}$	% ^b	$\Delta G_{\text{DGDZVP}}^{\text{e}}$	% ^f
1a	0.72	22.8	0.01	49.4	0.00	56.6	0.00	70.7
1b	0.00	77.2	0.00	50.6	1.16	43.4	0.52	29.3
5a	1.33	7.3	0.00	55.8	0.00	56.3	0.00	61.2
5b	1.74	3.6	0.18	41.1	0.17	42.3	0.29	37.4
5c	0.00	68.3	1.96	0.2	2.49	0.8	2.52	0.9
5d	0.70	20.8	2.38	0.1	2.70	0.6	2.76	0.5
6a	0.76	21.7	0.00	56.8	0.00	56.8	0.00	61.6
6b	0.00	78.3	0.16	43.2	0.16	43.2	0.28	38.4
7a	0.00	51.2	0.00	62.3	0.00	59.3	0.00	48.6
7b	0.45	23.7	0.36	34.0	0.27	37.7	0.02	47.0
7c	0.57	19.5	1.99	2.2	2.09	1.7	1.80	2.3
7d	1.31	5.6	2.22	1.5	2.26	1.3	1.84	2.1
8a	0.00	56.5	0.00	65.5	0.00	71.7	0.00	75.2
8b	0.16	43.5	0.38	34.5	0.55	28.2	0.66	24.8
9a	0.00	51.7	0.00	58.1	0.00	82.8	0.00	88.0
9b	0.19	37.5	0.25	38.0	1.02	14.9	1.61	5.9
9c	1.25	6.3	1.90	2.4	2.32	1.6	1.92	3.5
9d	1.45	4.5	2.13	1.6	2.85	0.7	2.07	2.6

^aRelative to **1b** (72.97 kcal/mol), **5c** (85.64 kcal/mol), **6b** (19.26 kcal/mol), **7a** (41.56 kcal/mol), **8a** (18.70 kcal/mol), and **9a** (40.43 kcal/mol).

^bCalculated using $\Delta E \cong -RT \ln K$.

^cRelative to **1b** (-722 568.44 kcal/mol), **5a** (-722 552.30 kcal/mol), **6a** (-385 257.39 kcal/mol), **7a** (-385 245.64 kcal/mol), **8a** (-385 257.93 kcal/mol), and **9a** (-385 246.26 kcal/mol).

^dRelative to **1a** (-722 658.13 kcal/mol), **5a** (-722 643.58 kcal/mol), **6a** (-385 308.14 kcal/mol), **7a** (385 296.01 kcal/mol), **8a** (-385 308.33 kcal/mol), and **9a** (-385 297.16 kcal/mol).

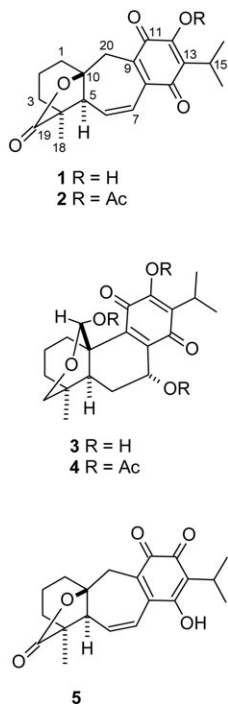
^eRelative to **1a** (-722 445.90 kcal/mol), **5a** (-722 432.24 kcal/mol), **6a** (-385 205.46 kcal/mol), **7a** (-385 193.98 kcal/mol), **8a** (-385 206.58 kcal/mol), and **9a** (-385 195.43 kcal/mol).

^fCalculated using $\Delta G = -RT \ln K$.

energy barrier seems to be relatively high. Therefore, bowl- and dome-shaped molecular structures for **2** and a single molecular structure of **4** were built in the Spartan 08 software followed by molecular mechanics force field search using the Monte Carlo methodology to provide four conformers for each shape of **2**, while for **4**, there were 12 conformers in a 6.92 kcal/mol energy gap. All conformers were submitted to single-point optimization using DFT at the B3LYP/6-31G(d) level of theory using the same software, from where the eight conformers of **2** were retained in a 2.94 kcal/mol gap, and six conformers in an energy gap of 1.82 kcal/mol correspond to **4**. These conformers were further optimized at the B3LYP/DGDZVP level of theory using the Gaussian 03 suit as indicated in Section 2. The final conformational optimization, IR and VCD calculations at the same level of theory were also performed using the Gaussian 03 software, the pertinent thermochemical parameters being summarized in Table 2. These thermochemical parameters are given in kcal/mol rather than in Hartrees since

mol is one of the seven basic units of science, which is defined from the exact numerical value of the Avogadro constant. Although the Gaussian 03 software provides these values in Hartrees, they were converted to kcal/mol using the factor 1 Hartree = 627.51 kcal/mol. Comparison of the calculated and experimental spectra, using the CompareVOA software,¹⁸ showed excellent agreement. The comparison parameters are summarized in Table 3, while the IR and VCD spectra are contrasted in Figure 2 for **2**, and in Figure 3 for **4**. It follows that the absolute configuration of icetexone acetate (**2**) and conacytone triacetate (**4**), and therefore of the diterpenes **1** and **3** are those drawn in Scheme 1.

The formulas of icetexone (**1**) and conacytone (**3**) reveal quite peculiar diterpenoids with the C-ring containing a hydroxyquinone chromophore and the A-ring supporting a fourth ring which is a heterocycle. Therefore, these molecules deserve detailed as possible ¹H and ¹³C NMR assignments. In particular, icetexone (**1**) possesses four methylene groups of which only the hydrogen atoms



SCHEME 1 Formulas of diterpenes originally reported from *Salvia ballotaeflora* and their acetates **2** and **4**

at C-20 appear as an amenable AB system, while the remaining three methylene groups at C-1, C-2, and C-3 of the A-ring should be coupled due to their vicinity. Thus, the one-dimensional (1D) ^1H and ^{13}C NMR spectra of **1** in combination with two-dimensional (2D) gHSQC and gHMBC measurements provided the data summarized in Section 2 in which all carbon atoms are ascribed individually together with the assessment of all hydrogen chemical shifts. However, determination of all homonuclear hydrogen coupling constants is precluded in the case of the A-ring atoms by the fact that three of them (H-1, H-2, and H-2') are completely overlapped, resonating at δ 1.81, and a fourth signal (H-3) appears quite close, at δ 1.77, providing a chemical shift difference of only 0.04 ppm, which at 300 MHz corresponds to 12 Hz, a value of similar magnitude than $^2J_{\text{gem}}$ or $^3J_{\text{trans}}$ in a conformational rigid cyclohexane.

In turn, conacytone (**3**) possesses the three A-ring methylenes and two further methylene arrangements, one at the heterocycle and the other one at the B-ring. A similar 1D and 2D NMR measurement procedure was applied for the signal assignment, thus providing all ^1H and ^{13}C chemical shift values, as well as some coupling constants. Since visual inspection of the ^1H spectrum reveals a higher dispersion of multiplets than in the case of **1**, and in order to assign the coupling constants of **3**, the raw ^1H NMR data were used as the starting point to achieve a complete and detailed assignment using the iterative full spin analysis integrated in the PERCH

(PERCH Solutions, Ltd., Kuopio, Finland) v.2011.1 NMR software,²⁴ a methodology we have successfully used for the complete spectra assignment of some natural products.^{25,26} The method is based on the iterative minimization of the differences found between the simulated and the experimental spectra to determine the total ^1H NMR data for the studied molecule. Therefore, the 300 MHz free induction decay of **3** was edited in the preparation (PAC) module of the software, while the molecular structure of the minimum energy conformer was imported into the molecular modelling software (MMS) module, also of the PERCH shell. In addition, all chemical shift values and the directly observed coupling constants were introduced in the parameter table. These data allowed undertaking iteration processes until a convergence between the experimental and calculated spectra reached a RMS of 0.080%. All ^1H chemical shifts and coupling constants are summarized in Table 1, although it should be noted that in this case, the software was unable to distinguish the *pro-R* and *pro-S* methyl signals of the isopropyl residue, probably due to the very small chemical shift difference of only 0.005 ppm and a free rotation about the C-13/C-15 single bond. Of relevance to observe are a couple of four bonds long-range coupling constants one owing to each hydrogen atom at C-19, H-19_{*pro-R*} being coupled to H-3 α , and H-19_{*pro-S*} to H-5. Of relevance to note is also that $^2J_{\text{gem}}$ of the methylene hydrogen atoms at C-1, C-2, C-3, and C-6 is -13.3 ± 0.4 Hz, while $^2J_{\text{gem}}$ of the heterocyclic C-19 methylene atoms is -11.2 Hz due to the electronegativity of the directly attached oxygen atom. Due to the fact that PERCH calculations afford chemical shifts with six and coupling constants with four decimal places, and since the experimental 300 MHz spectrum was acquired with a magnet homogeneity better than 0.14 Hz, the chemical shifts and coupling constant values with three and two digits after a decimal point, respectively, given in Table 1, constitute a proper description, as has previously^{27,28} been done. A detailed comparison of the individual multiplets of the experimental and calculated ^1H NMR spectra of **3** is shown in Figure 5.

Once the complete assignment of the NMR data of conacytone is at hand, and thanks to a reviewer observation, it follows that the data agree with those of an oily molecule named turbinatone,²⁹ which was isolated from *Eupatorium turbinatum*, to which structure **3** was assigned independently. In addition, **3** was also detected recently³⁰ in *Salvia corrugata*.

The ^{13}C NMR substituent chemical shift (SCS) parameters for quinones, which we determined a long time ago²⁹ using monoterpenes and monocyclic sesquiterpenes, were evaluated in the present study which constitutes an opportunity to test these parameters for diterpenes in which the quinone ring is fused to another

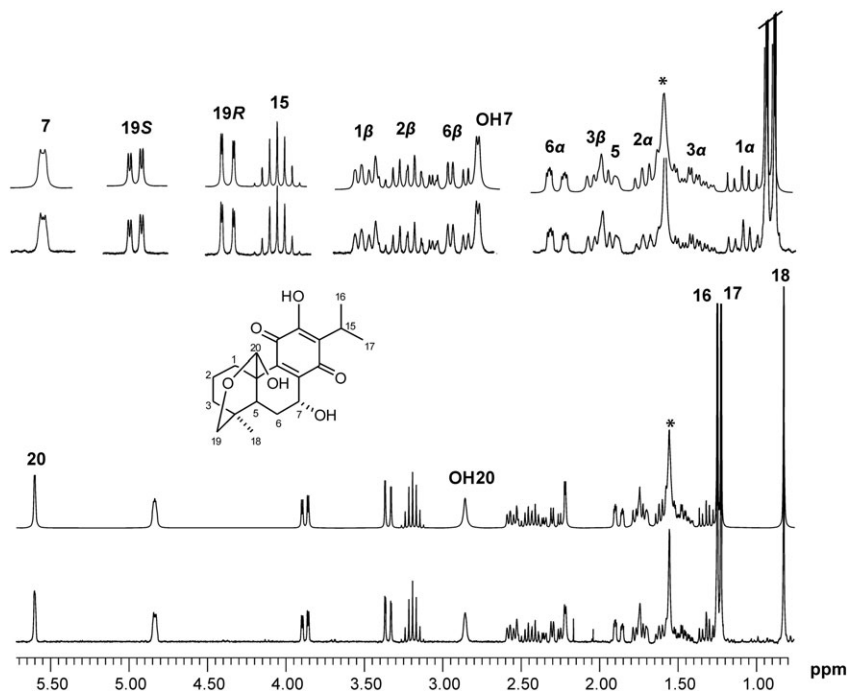


FIGURE 5 Comparison of the PERCH calculated (top) and the experimental (bottom) 300 MHz ^1H NMR spectra of conacytone (**3**). The labeled peak (*) is due to moisture

carbocycle. Table 5 shows the literature values for chloroform solutions, which differ from those for DMSO solutions,³¹ together with the chemical shift changes induced for the **1** to **2** and the **3** to **4** transformations. It can be seen that in the case of icetexone (**1**) and its acetate **2**, the SCS values agree excellently, the same being true for C-11, C-12, and C-13 on going from conacytone (**3**) to its triacetate **4**, while for C-8, C-9, and C-14, there is a lack in agreement. This seems to be due to the presence of the C-7 and C-20 acetates as can be observed in the minimum energy conformers of **4** shown in Figure 4.

Close inspection of the formulas of icetexone (**1**) and romulogarzone (**5**) reveals that these molecules are tautomers, an unprecedented situation for their coexistence as natural products, which generates a case that must be proven rigorously to ascertain if such a coexistence is feasible. Since there is no way to do experimentation

with a substance we have been unable to isolate over the years, to which formula **5** was proposed,⁴ we resorted to theoretical studies. Given our over one-half a century experience with the natural occurring sesquiterpene benzoquinone perezone,³²⁻³⁷ which possesses a 2-hydroxy-1,4-benzoquinone chromophore as in **1**, we consider the existence of the 4-hydroxy-1,2-benzoquinone tautomer **5** as energetically extremely disfavored, among other reasons, since the hydrogen bonding in a 2-hydroxy-1,4-benzoquinone significantly favors this atom arrangement.

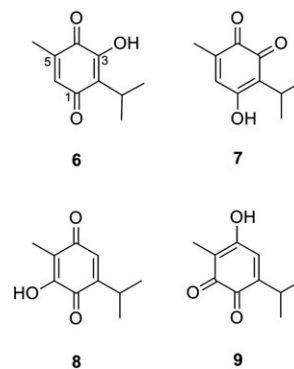
In order to test this hypothesis in a preliminary way, without investing significant computer times for keto/enol tautomerism, we initially resorted to calculate small monoterpenoid quinones with which we are familiar,³¹ and therefore selected (Scheme 2) 3-hydroxythymoquinone (**6**) and 6-hydroxythymoquinone

TABLE 5 Acetylation-induced ^{13}C NMR substituent chemical shift parameters^a

Effect at	Literature ^b	1 and 2	3 and 4
Adjacent CO	-3.5 ± 0.2	-3.6	-3.7
Remote CO	-0.6 ± 0.1	-0.2	-3.7
ipso	-1.9 ± 0.1	-1.9	-1.8
ortho	$+15.6 \pm 0.3$	+15.4	+15.1
meta	$+3.0 \pm 0.7$	+3.4	-2.6
para	-1.7 ± 1.1	-0.6	+1.4

^aFor CDCl_3 solutions.

^bFrom Burgueño-Tapia and Joseph-Nathan.³¹



SCHEME 2 Formulas of 3- (**6**) and 6-hydroxythymoquinone (**8**) and their tautomers **7** and **9**

(8) in order to compare their free energies with those of their 4-hydroxy-1,2-benzoquinones **7** and **9** tautomers, respectively, since these are C₁₀H₁₂O₃ molecules containing only 96 electrons. Inspection of Table 4 reveals that both **6** and **8** provide two energetically relevant conformers due to rotation of the isopropyl group, while each **7** and **9** provide four relevant conformers due to rotation of both the isopropyl group and the hydroxy group, since in the *ortho*-quinones, the latter is no longer hydrogen bonded to a carbonyl group. Thus, determination of the free energy of the most stable conformer of **6-9** using DFT calculations at the B3LYP/DGDZVP level of theory revealed that for these monoterpenoids, the values were -385205.46, -385193.98, -385206.58, and -385195.43 for **6**, **7**, **8**, and **9**, respectively, from where it follows the difference between 2-hydroxy-1,4-thymoquinones and their 4-hydroxy-1,2-quinone tautomers lies in the order of 11 kcal/mol. In fact, $\Delta G_7 - \Delta G_6 = 11.5$ kcal/mol, and $\Delta G_9 - \Delta G_8 = 11.2$ kcal/mol. Although this energy difference is in the order of the barrier for the interconversion of cyclohexane, it is a very high value for keto/enol tautomerism where only electrons and a hydrogen atom are relocated. Encouraged by these results, we calculated the free energies of the most stable conformers of icetexone (**1**) and romulogarzone (**5**), which were -722445.90 and -722432.24, respectively (Table 4) providing $\Delta G_5 - \Delta G_1 = 13.7$ kcal/mol. Therefore, according to the $\Delta G = -RT \ln K$ equation, solved for two tautomer molecules in equilibrium, the relative abundance of **5:1** would be around one part of **5** per one hundred billion (1×10^{11}) parts of **1**. Although this extremely low abundance of **5** is not violating the Avogadro constant, for practical purposes, it allows to declare, 41 years after its launch, that romulogarzone (**5**) is inexistent.

4 | CONCLUSION

Although icetexone (**1**) and conacytone (**3**) were originally isolated in 1976, no detailed assigned NMR characterization of either very peculiar diterpenoid is available nor has the absolute configuration of these molecules been established rigorously. Therefore, we determined all ¹³C and ¹H NMR chemical shifts of **1-4** and were able to also determine all hydrogen homonuclear coupling constants of conacytone (**3**). We also determined the crystal X-ray structure of **1** and **3**, whose Flack and Hooft parameters provided the absolute configuration, which was further tested by comparison of experimental VCD spectra of the derived acetates **2** and **4** with those obtained by DFT calculations at the B3LYP/DGDZVP level of theory. The known SCS values for hydroxy-*p*-benzoquinones were contrasted with the chemical shift differences induced

upon acetylation of icetexone (**1**) and conacytone (**3**). It follows that for **1**, all SCS values are in excellent agreement, while for **3**, those of C-11, C-12, and C-13 agree very well, while for the remaining three quinone ring carbons, there is no agreement due to the introduction of additional acetyl groups at C-7 and C-20. Finally, DFT calculations at the B3LYP/DGDZVP level of theory provide conclusive evidence that romulogarzone (**5**), the third diterpenoid claimed to occur in nature together with icetexone (**1**) and conacytone (**3**), cannot exist since tautomer **1** is more stable than **5** by 13.7 kcal/mol, which is a huge energy amount for keto/enol tautomerism.

ORCID

Pedro Joseph-Nathan  <http://orcid.org/0000-0003-3347-3990>

REFERENCES

1. Domínguez XA, González H. Extractives from *Salvia ballotaeflora*. *Phytochemistry*. 1972;11:2641-2641.
2. Watson WH, Taira Z, Domínguez XA, González H, Gutiérrez M, Aragón R. Isolation and structure of two diterpene quinones from *Salvia ballotaeflora* Benth (Labiatae). *Tetrahedron Lett*. 1976;2501-2502.
3. Taira Z, Watson WH, Domínguez XA. Structure of icetexone, a diterpene quinone from *Salvia ballotaeflorae*. *J Chem Soc Perkin Trans*. 1976;2:1728-1730.
4. Domínguez XA, González H, Aragón FR, Gutiérrez M, Marroquín JS, Watson W. Mexican medicinal plants XXIX. Three new diterpene quinones from *Salvia ballotaeflora*. *Planta Med*. 1976;30:237-241.
5. Taira Z, Watson WH. The structure of conacytone, C₂₀H₂₆O₆, a diterpene quinone from *Salvia ballotaeflorae*. *Acta Crystallogr*. 1976;B32:2149-2152.
6. Sánchez C, Cárdenas J, Rodríguez-Hahn L, Ramamoorthy TP. Abietane diterpenoids of *Salvia anastomosans*. *Phytochemistry*. 1989;28:1681-1684.
7. Cárdenas J, Rodríguez-Hahn L. Abietane and icetexane diterpenoids from *Salvia candicans*. *Phytochemistry*. 1995;38:199-204.
8. Esquivel B, Calderón JS, Flores E, Chávez C, Juárez M. Abietane and icetexane diterpenoids from *Salvia pubescens*. *Nat Prod Lett*. 1997;10:87-93.
9. Majetich G, Grove JL. Total synthesis of (+)-19-deoxyicetexone, (-)-icetexone, and (+)-5-*epi*-icetexone. *Org Lett*. 2009;11:2904-2907.
10. Cortez FJ, Lapointe D, Hamlin AM, Simmons EM, Sarpong R. Synthetic studies on the icetexones: enantioselective formal syntheses of icetexone and *epi*-icetexone. *Tetrahedron*. 2013;69:5665-5676.

11. Galicia MA, Esquivel B, Sánchez AA, Cárdenas J, Ramamoorthy TP, Rodríguez-Hahn L. Abietane diterpenoids from *Salvia pubescens*. *Phytochemistry*. 1988;27:217-219.
12. Esquivel B, Calderón JS, Flores E, Sánchez AA, Rivera RR. Abietane and icetexane diterpenoids from *Salvia ballotaeflora* and *Salvia axillaris*. *Phytochemistry*. 1997;46:531-534.
13. Farrugia LJ. WinGX suite for small-molecule single-crystal crystallography. *J Appl Cryst*. 1999;32:837-838.
14. Dolomanov O, Bourhis LJ, Gildea RJ, Howard JAK, Puschmann H. OLEX2: a complete structure solution, refinement and analysis program. *J Appl Cryst*. 2009;42:339-341.
15. Parsons S, Flack HD, Wagner T. Use of intensity quotients and differences in absolute structure refinement. *Acta Crystallogr*. 2013;B69:249-259.
16. Hooft RWW, Straver LH, Spek AL. Using the t-distribution to improve the absolute structure assignment with likelihood calculations. *J Appl Cryst*. 2010;43:665-668.
17. Hooft RWW, Straver LH, Spek AL. Determination of absolute structure using Bayesian statistics on Bijvoet differences. *J Appl Cryst*. 2008;41:96-103.
18. Debie E, De Gussem E, Dukor RK, Herrebout W, Nafie LA, Bultinck P. A confidence level algorithm for the determination of absolute configuration using vibrational circular dichroism or Raman optical activity. *Chemphyschem, Special Issue: Jacobus van't Hoff*. 2011;12:1542-1549.
19. Ortega AR, Toscano RA, Hernández-Barragán A, Alvarez-Cisneros C, Joseph-Nathan P. Structure elucidation of a new isoflavone by exclusive use of ¹H NMR measurements. *Magn Reson Chem*. 2015;53:860-865.
20. Joseph-Nathan P, Gordillo-Román B. Vibrational circular dichroism absolute configuration determination of natural products. In: Kinghorn AD, Falk H, Kobayashi J, eds. *Progress in the Chemistry of Organic Natural Products*. Vol.100 Switzerland: Springer International Publishing; 2015:311-451.
21. Burgueño-Tapia E, Joseph-Nathan P. Vibrational circular dichroism: recent advances for the assignment of the absolute configuration of natural products. *Nat Prod Commun*. 2015;10:1785-1795. 2017;12:641-651
22. Burgueño-Tapia E, Joseph-Nathan P. Absolute configuration of eremophilanoids by vibrational circular dichroism. *Phytochemistry*. 2008;69:2251-2256.
23. Burgueño-Tapia E, Sánchez-Castellanos M, Joseph-Nathan P. Optimization of the considered number of conformers for the absolute configuration determination of catechin and epicatechin peracetates by VCD. *Nat Prod Commun*. 2017;12:683-686.
24. Laatikainen R, Tiainen M, Korhonen S-P, Niemitz M. Computerized analysis of high-resolution solution-state spectra. In: Harris RK, Wasylishen RE, eds. *Encyclopedia of Magnetic Resonance*. Chichester: Wiley; 2012:677-688.
25. Molina-Salinas GM, Rivas-Galindo VM, Said-Fernández S, et al. Stereochemical analysis of leubethanol, an anti-TB-active serrulatane from *Leucophyllum frutescens*. *J Nat Prod*. 2011;74:1842-1850.
26. Villanueva-Cañongo C, Pérez-Hernández N, Hernández-Carlos B, Cedillo-Portugal E, Joseph-Nathan P, Burgueño-Tapia E. Complete ¹H NMR assignments of pyrrolizidine alkaloids and a new eudesmanoid from *Senecio polypodioides*. *Magn Reson Chem*. 2014;52:251-257.
27. Becerra-Martínez E, Ramírez-Gualito KE, Pérez-Hernández N, Joseph-Nathan P. Total ¹H NMR assignment of 3 β -acetoxypregna-5,16-dien-20-one. *Steroids*. 2015;104:208-213.
28. Ortega AR, Ortiz-Pastrana N, Quijano L, Becerra-Martínez E, Olmedo-Aguirre JO, Joseph-Nathan P. Structure and absolute configuration of hydroxy-bis-dihydrofarinosin from *Encelia farinosa*. *Magn Reson Chem*. 2017;55:530-539.
29. Jakupovic J, Ellmauerer E, Bohlmann F, Whitemori A, Gage D. Diterpenes from *Eupatorium turbinatum*. *Phytochemistry*. 1986;25:2677-2678.
30. Bisio A, Fraternali D, Schito AM, et al. Establishment and analysis of *in vitro* biomass from *Salvia corrugata* Vahl. and evaluation of antimicrobial activity. *Phytochemistry*. 2016;122:276-285.
31. Burgueño-Tapia E, Joseph-Nathan P. ¹³C NMR substituent chemical shifts in hydroxy-*p*-benzoquinones. *Magn Reson Chem*. 2000;38:390-393.
32. Walls F, Salmón M, Padilla J, Joseph-Nathan P, Romo J. La estructura de la perezona. *Bol Inst Quím Univ Nal Autón Méx*. 1965;17:3-15.
33. Joseph-Nathan P, Reyes J, González MP. Contribution to the chemistry of perezona. *Tetrahedron*. 1968;24:4007-4013.
34. Joseph-Nathan P, Martínez E, Rojas M, Santillan RL. The solid state versus the solution structure of 6-hydroxyperezona. *J Nat Prod*. 1987;50:860-865.
35. Joseph-Nathan P, Santillan RL. The chemistry of perezona and its consequences. In: Atta-ur-Rahman, ed. *Studies in Natural Products Chemistry*. Vol.5 Amsterdam: Elsevier; 1989:763-813.
36. Burgueño-Tapia E, Cerda-García-Rojas CM, Joseph-Nathan P. Conformational analysis of perezona and dihydroperezona using vibrational circular dichroism. *Phytochemistry*. 2012;74:190-195.
37. Zepeda LG, Burgueño-Tapia E, Pérez-Hernández N, Cuevas G, Joseph-Nathan P. NMR-based conformational analysis of perezona and analogues. *Magn Reson Chem*. 2013;51:245-250.

How to cite this article: Esquivel B, Burgueño-Tapia E, Bustos-Brito C, Pérez-Hernández N, Quijano L, Joseph-Nathan P. Absolute configuration of the diterpenoids icetexone and conacytone from *Salvia ballotaeflora*. *Chirality*. 2018;30:177-188. <https://doi.org/10.1002/chir.22781>